SCC-DFTB Study for the Structural Analysis of Crystalline Molecular Compasses

Anant Babu Marahatta[1, 2,]*, Hirohiko Kono[3]

[1]Department of Chemistry, Amrit Science Campus, Tribhuvan University, Kathmandu, Nepal
[2]Engineering Chemistry Unit, Department of Civil Engineering, Kathford International College of Engineering and Management (Affiliated to Tribhuvan University), Kathford International Education & Research Foundation, Kathmandu, Nepal
[3]Department of Chemistry, Graduate School of Science, Tohoku University, Sendai, Japan
*Corresponding author: abmarahatta@gmail.com

Abstract Over the last few decades, creating, modifying, and strategically synthesizing/designing nanomaterials along with their proper functionalization have gained the greatest admiration. These are in fact quite mandatory credentials of nanotechnology where science, engineering, and technology are interconnected just for manipulating the atoms and molecules at nanoscale range. Amid various types of emerging nanomaterials, the experimentally synthesized phenylene- bridged amphidynamic type crystalline macrocyclic molecular compounds having peripherally distributed static spokes have attracted substantial attentions in recent years. In the same context, we have reported a series of DFT, and DFT−based quantum mechanical, viz. SCC− & NCC− DFTB investigations of the crystal structures and the rotary dynamics of experimentally synthesized gyroscope−like amphidynamic type crystalline siloxaalkane macrocages with completely closed structural topology. Based on the performance of these theoretical models, herein, we simply employed SCC−DFTB scheme and explored unit−cell structures followed by the complete interpretation of the experimentally reported structural deformation of the exactly same type molecular gyroscopes but having diflouro (ROT−2F) and dichloro (ROT−2Cl) substituting dipolar rotating units (compass−needle) in the crystalline state. The synthetic structural molecular analogue of them having a central nonsubstituted phenylene unit as a rotator (ROT−2H) is taken here as a reference molecule. The general results presented here depict semiquantitatively reproduced X−ray observed crystal structures and the closely associated structural parameters for all the three molecular gyroscopes/compasses.

Keywords DFTB, Molecular Compass/Gyroscope, Dipolar Rotators, Amphidynamic Crystal

1. Introduction

Despite the availability of an exact DFT−based computational mean in characterizing ground state electronic structures of the multi−electron and/or many−body systems [1−4], its approximate mathematical variants, inability to integrate the exchange interactions correctly, failure to cope with the strongly correlated systems etc. have made itself far from fail−safe [5−10]. Besides these, there is a lack of proper and efficient mathematical formulations in DFT for accounting significant effect of long−range interactions or van der Waals (hereafter, vdW) type intra−/inter− molecular interactions existing predominantly in caged type crystalline macrocyclic molecular compounds (hereafter, CMMCs) with closed topology (**Chart−1**). More critically, to our experience, DFT computed relatively less efficiently or mostly turned out to be "failure" in computing low energy ground state electronic structures while

applying to such type macrocyclic molecular assemblies with bridged delocalized π−electron systems (**Fig. 1−2**) where vdW force competes significantly with other type molecular interactions in crystalline state. Over the period of this decade, in computing as reliable molecular structures as DFT efficiently, and in characterizing the crystalline molecular geometry more appropriately, the relatively less computationally complex yet highly competent density functional based tight binding (hereafter, DFTB) scheme implemented in the DFTB+ program package has been heavily extended to CMMCs mainly to perform specific type calculations over long timescales under both periodic and isolated molecular conditions [11−15]. This scheme is actually based on the DFT but is formulated uniquely so as to execute Slater−Kirkwood model [16] and the Slater−Koster files (hereafter, SK files) [17] efficiently with a primary focus on giant periodic molecular assemblies held together by dispersion type forces. Even though it uses pre−calculated parameters, a minimal basis, and includes only the nearest−neighbor interactions, it computes DFT−level results at an extremely low computational cost. In order to drive specific type computations, the DFTB+ package has offered (a) non−self-consistent−charge DFTB (hereafter, NCC−DFTB) [12−14], and (b) self-consistent−charge DFTB (hereafter, SCC−DFTB) source codes [18,19] based on the zeroth− and second− order expansions of the DFT Kohn−Sham energy with respect to charge density fluctuations respectively. These codes are mainly designed just to bring off Slater− Kirkwood model and SK−files computationally, leading themselves towards incorporating and executing the substantial effect of vdW type molecular interactions with the inclusion of some predefined logical approximations [20−22]. However, the latter DFTB scheme is mostly recognized as a promising computational approach due to its ability to account for the Mulliken charge distributions and atomic charge interactions through iterative self-consistent manner [18, 19], owing to present itself as a unique SCC approach suits for computing accurate ground state electronic structures of the heteroatomic complex and giant molecular systems in crystalline state (**Fig. 1−2**) [21, 22].

To the knowledge of these authors, the most significant reason behind the wide recognition of phenylene bridged CMMCs with peripherally distributed flexible arms (**Fig. 1−2**) as the most potential candidates for nanotechnology is due to their unique amphidynamic feature: the central phenylene unit (*i.e.* rotator) of each molecule in the crystalline assembly rotates internally with respect to its own stationary spokes (*i.e.* stator) at high to moderate temperatures ranges [23−25]. This feature is in fact highly expected as a functionalized property more especially while developing/creating ambitious yet realistic type smart, responsive, and intelligent nanomaterials. More preferentially, the strategically designed CMMCs with enough free space (free−volume unit) around the rotating phenylene units attaching polar substituents such as fluoro−, chloro−, cyano−, amino−, nitro−, nitroamino−, diamino−, etc. are highly anticipated to demonstrate externally controlled rotary motion along with conserving internal volume [26, 27]. In fact, the solid−state crystalline molecular compounds with such dipolar substituents or compass needle on the central rotating unit are called molecular compass in analogous to macroscopic compass used for navigation and geographic orientation. Structurally, just like in macroscopic compass, the central dipolar rotator of the molecular compass is linked to the 1, 4−axial positions themselves are connected to the stationary spokes externally [23]. In nanotechnology, such type crystalline molecular assemblies are expected to be functionalized realistically as they may show comparatively far better controlled rotary motion and unidirectional rotation while applying external stimuli such as static electric field, magnetic field, light etc. Actually, these stimuli can reorient the central compass−needles resulting the variation of the optical properties such as dichroism and birefringence [26−29] which could be an indispensable feature of the newly invented nano−devices. The research group led by Prof. W. Setaka has experimentally synthesized different types of gyroscope like Si−based crystalline molecular compounds (hereafter, siloxaalkane molecular gyroscope) (**Fig. 1−2**) with dipolar (halogen substituted) and nonpolar (nonsubstituted) phenylene rotators encapsulated inside the three different siloxaalkane spokes [23, 24]: the molecular gyroscopes with phenylene rotators, hereafter called ROT−2H (**1a**, **Fig. 1**), and the molecular compasses with difluorophenylene & dichlorophenylene rotators, hereafter called ROT−2F (**1b**, **Fig. 2a**) and ROT−2Cl (**1c**, **Fig. 2b**) respectively.

Chart 1#
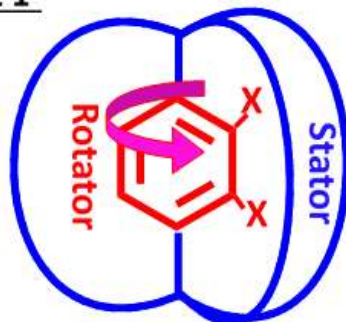
1a; X = H (ROT-2H)
1b; X = F (ROT-2F)
1c; X = Cl (ROT-2Cl)

#It is a model of the amphidynamic type crystalline macrocyclic molecular compounds (CMMC) with completely closed structural topology. All the groups and atoms that construct the surrounding arms are omitted for clarity.
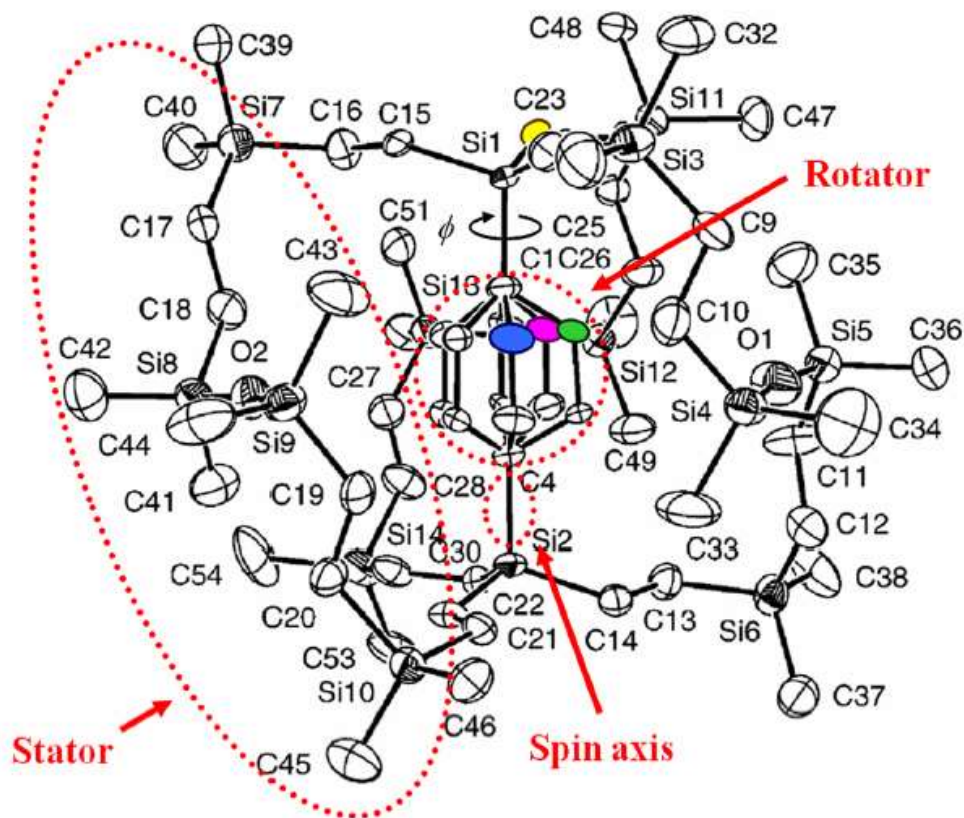

Figure 1: X-ray crystallography of the crystalline molecular gyroscope 1a (ROT-2H) with three stable phenylene positions A, B & C (indicated by blue, pink, and green spheroids) inside the siloxaalkane spokes. It is taken from the supporting information of ref 23. The phenylene dihedral angle is formed by C23 (yellow colored spheroid)-Si1-C1-ortho C atom (other colored spheroids).

Interestingly, they observed ROT−2H and ROT−2F as amphidynamic crystals with a periodic lattice having C_2 symmetry (2−fold symmetry axes) through the X−ray crystallography: the concerned rotators of them were observed to flip in between three (position **A**, **B**, and **C**), and two (position **A** and **B**) stable positions respectively inside the static siloxaalkane spokes. In contrast to this, ROT−2Cl has no symmetry, and was observed as non−amphidynamic crystal with a rigid dichlorophenylene unit and the static yet significantly deformed siloxaalkane frame structure.

Owing to the application of DFT and DFT−based computational models (NCC− and SCC− DFTB) to all these experimentally synthesized crystalline molecular gyroscopes **1a**, **1b**, and **1c** separately under isolated molecular conditions, we achieved as reliable results as X−ray crystallography [20, 21, 30, 31]. More particularly, we found these methods consistently good for geometries, energies, and the rotary dynamics of the molecular gyroscope **1a** under crystalline molecular conditions [20, 21]. Accordingly, we recognized them as quite able theoretical methods in order to predict as accurate ground state electronic structures as DFT under isolated molecular condition while applying to the molecular compasses **1b** and **1c** [30, 31]. In regard to these complex yet valuable theoretical investigations, we further applied SCC−DFTB scheme to **1b** and **1c** molecular compasses under crystalline condition, and computed their crystal structures quantum mechanically. In this contribution, we have reported mainly the SCC−DFTB predicted crystal structures of experimentally synthesized **1b** and **1c** molecular compasses and their theoretical interpretations. Additionally, herein, we have theoretically inquired and quantified experimentally observed structural and dynamical effects of the deformed siloxaalkane spokes in confining dipolar diflouro− (as in **1b**) and dichloro− (as in **1c**) phenylene rotators at the specific positions. For their structural comparisons, the X− ray produced, and the SCC−DFTB optimized unit−cell geometries of the molecular gyroscope **1a** are referred here due to being latter as their structural analogy and precursor module during laboratorial synthetic processes.

The entire structure of this research report is as follows. The theoretical approaches and computational methods are outlined in section 2, the relevant results are discussed in section 3, and the concise conclusions are presented in section 4.

2. Computational Details

Prior to compute low energy electronic structures of each crystalline molecular compound **1a**, **1b**, and **1c** under periodic boundary condition (hereafter, PBC), the X−ray crystallographic data for each of them was critically analyzed and extracted the concerned unit cell Cartesian coordinates and the respective lattice parameters a, b, c (lengths of the unit cell in three dimensions) and α, β, γ (three interaxial angles). In the case for **1a**, the Cartesian coordinates of the unit cell of its most stable structure **B** (dihedral angle $\phi = 0.55\pi$, **1a** has three X−ray observed stable structures **A**, **B**, and **C**) at 223 K (monoclinic crystal, number of molecules per unit cell = 2); for **1b**, the unit cell coordinates of both of its X−ray observed degenerate stable structures **A** (dihedral angle $\phi = 0.56\pi$) & **B** (dihedral angle $\phi = 1.57\pi$) at 273 K (orthorhombic crystal, number of molecules per unit cell = 4); and for **1c**, the unit cell coordinates of its single stable structure (dihedral angle $\phi = 0.61\pi$) at 273 K (orthorhombic crystal, number of molecules per unit cell = 2) were taken as their trial structures. Since the dihalogen substituted molecular gyroscopes **1b** and **1c** are the molecular analogues of the precursor molecule **1a**, the latter one was considered here as a reference molecule whose most stable equilibrium structure "position **B**" with dihedral angle $\phi = 0.55\pi$ was used as trial structure and optimized it under crystalline condition, whereas for the molecular gyroscope **1b**, both of its X−ray derived degenerate equilibrium unit cell structures "position **A** with dihedral angle $\phi = 0.56\pi$" and "position **B** with dihedral angle $\phi = 1.57\pi$" that vary to each other by 1π difluorophenylene flipping were optimized. Contrastingly, being **1c** a non−amphidynamic type crystal due to possessing a rigid dichlorophenylene unit in the central position, a single stable unit cell X−ray geometry of it was optimized. The latter optimization was actually carried out for the purpose of quantifying the degrees of structural deformation theoretically that was experimentally observed more especially in the surrounding siloxaalkane spokes of **1c** while accommodating comparatively more bulky phenylene unit (Cl−substituted) centrally. We employed DFTB+ optimizer for determining the ground state electronic crystal structures of each molecular gyroscope/compass at an extremely low computational cost but with considerable precisions. While displaying their unit cell structures individually in the three dimensional axes under crystalline molecular condition, we used specifically designed open− source *Java* viewer *Jmol* [32]. Accordingly, the *Jmol:* measurements features were used to determine all the structural parameters such as bond lengths, bond angles, dihedral angles, free − volume units etc. of each optimized unit cell.

The DFTB+ script was edited based on the requirements of the present theoretical calculations. Likewise, the geometry−optimizer codes were modified by inserting proper DFTB keywords mentioned in the users' manual available elsewhere [33]. The Hamiltonian and the molecular crystalline conditions were imposed *via* the keywords "Hamiltonian = DFTB" and "Periodic = Yes, LatticeOpt = Yes". For Brillouin zone integration, the special k−points and their weights in integral were specified explicitly under "KPointsAndWeights". Each trial structure of the unit cell was described by the Cartesian coordinates of the atoms in the XYZ format through the keyword "GenFormat". For altering the geometry of the input structure while the quantum mechanical calculations were on the fly, the "Conjugate gradient algorithm" was selected as a driver with a force component "ForceComponent = $1e$−4" as its maximal absolute value for controlling the optimization process. No any geometry constraints were applied *i.e.* all the atoms of the unit cell were allowed to move freely during the optimization steps. Similarly, for monitoring whether the calculations were proceeded normally or not, the geometry component "AppendGeometries = Yes" was set which in fact creates a file (in XYZ format) listing out all the recurring geometries obtained through optimizations; and for ensuring the DFTB+ script to run SCC type calculations, the "ConvergentForcesOnly" keyword was set to "SCC = YES" so that the prematurely stopped geometry optimizations can be controlled whenever the SCC cycle does not converge at any geometric step. The stopping criteria for the SCC and the maximal number of SCC cycles to reach the convergence limit were fixed to $1e$−4 and 200 respectively through their respective keywords "SCCTolerance" and "MAXSCCIterations". Additionally, while evaluating the dispersion energy corrections mathematically, a Slater−Kirkwood polarization atomic model [16, 33] was called *via* the keyword "Dispersion = SlaterKirkwood". This model was actually implemented to enable the DFTB+ script for incorporating the vDW type intramolecular interactions between the phenylene rotator and the siloxaalkane spokes plus intermolecular interactions between the periodically arranged molecules. The required dispersion constants for running this model such as polarizabilities α (Å^3), Slater−Kirkwood effective numbers N_{eff} of the electrons, cutoff interaction range r_c (Å), and the charge (Chrg.) for each and every atoms having unique coordination were supplied through "HybridDependentPol" tag. The covalent radii for each atomic species were specified using the "CovalentRadius" keyword which is then followed by a "HybridPolarisations" block containing a list of specific values for these parameters. The concerned values for them were taken from the previous publications of the same authors [20, 33] where proper validations and testing of the parameter sets for H, C, O, Si atoms are explained in reference to the crystalline molecular gyroscope **1a**. The dispersion constants for the halogen atoms F and Cl were calculated based on the mathematical procedures mentioned elsewhere [34], [35]. Furthermore, to execute the model computationally, the Slater−Koster files with a focus on solid state systems were explicitly used from the *mio−1−1* and *pbc−0−3* sets for every pairwise permutation atomic types [17, 33].

3. Results and Discussions

In reference to our previously published research works reported elsewhere [20−22, 30, 31], we realized the SCC−DFTB optimizer as a superb computational procedure because of its efficient ability to run self−consistent type calculation of the Mulliken charges and to derive the corresponding nuclear forces at exceptionally low computational cost. This feature actually makes the DFTB very useful more specifically to the solid state heteroatomic giant molecular systems where charge balance between the atoms are considered seriously during specific type calculations.

In this study, we computationally optimized the X−ray nuclear coordinates of all the three molecular gyroscopes/compasses **1a**, **1b**, and **1c** under periodic boundary condition (crystalline molecular assembly) without any geometric constraints using SCC−DFTB method, and interpreted the theoretically produced equilibrium structures on the basis of their X−ray derived molecular geometries. At first, the X−ray produced most stable unit cell structure (Figure 3(a)) of the crystalline molecular gyroscope **1a** was optimized fully without any geometric constraints under PBC followed by the similar type computations on the unit cell geometries of two different degenerate X−ray structures **A** (Figure 4(a)) and **B** (Figure 5(a)) for **1b**, and of a single stable unit cell structure for **1c** (Figure 6(a)) separately.

Table 1. Experimental vs. Theoretical structural parameters for the molecular gyroscopes **1a**, **1b**, and **1c** in their unit cell structures

Molecular Gyroscopes	Phenylene with spinning axes: Bonds	Bond length (Å)		"Free volume" $d_{CO}\{d_1, d_2, d_3\}$ (Å)		Rotator dihedral angle ϕ (π)	
		Expt.	SCC–DFTB	Expt.	SCC–DFTB	Expt.	SCC–DFTB
1a (ROT–2H)	C–C	1.41	1.41				
	C–H	0.94	1.10	3.9	4.1		
	C–Si$_1$	1.81	1.82	4.3	4.1	0.55	0.35
	C–Si$_2$	1.81	1.82	5.1	5.3		
1b (ROT–2F) (**Position A**)	C–C	1.36	1.41				
	C–F	1.44	1.41	5.9	5.6		
	C–H	0.93	1.10	8.5	7.9	0.56	0.60
	C–Si$_1$	1.89	1.87	8.1	7.7		
	C–Si$_2$	1.89	1.87				
(**Position B**)	C–C	1.36	1.41				
	C–F	1.44	1.41	5.9	5.9		
	C–H	0.93	1.10	8.5	7.9	1.57	1.61
	C–Si$_1$	1.89	1.87	8.1	7.8		
	C–Si$_2$	1.89	1.87				
1c (ROT–2Cl)	C–C	1.39	1.41				
	C–Cl	1.74	1.41	7.1	6.8		
	C–H	0.93	1.10	8.1	8.0	0.61	0.64
	C–Si$_1$	1.91	1.87	7.8	7.9		
	C–Si$_2$	1.89	1.87				

All these SCC–DFTB produced low energy electronic structures are displayed in Figure 3(b), Figure 4(b), Figure 5(b), and Figure 6(b) respectively. In order to depict these theoretically converged equilibrium unit cell structures quantitatively, and to assure whether they represent truly the ground state electronic structures or not in reference to the X–ray crystallographic structures, an exact determination and the accurate specification of the concerned structural parameters such as bond lengths, bond angles, dihedral angles, free–volume units etc. are very needful. Actually, in theoretical/computational chemistry, these chemical bonds and the molecular structure related parameters are very essential while locating the accurate position of the atomic nuclei that are associated with the 3D molecular geometries. Therefore, in this study, the mostly preferred structural parameter sets are carefully selected, and the SCC–DFTB generated unit cell equilibrium structures of all the three molecular gyroscopes **1a**, **1b**, and **1c** are analyzed thoroughly. The concerned SCC–DFTB computed values for the substituted and unsubstituted phenylene rotator are listed in Table 1 where the respective X–ray produced structural parameter values are also presented. We critically analyzed all the C−C bond lengths of both non−substituted and dihalogen (X = F and Cl) substituted phenylene units of **1a**, **1b**, and **1c** respectively, and are found them longer than the length of a standard C=C double bond as in ethylene (bond length = 1.34 Å) but shorter than that of a standard C−C single bond as in ethane (bond length = 1.47 Å). In the average range, all the pheylene C−C bond lengths are theoretically estimated as 1.40 Å; a standard value in benzene. It suggests us that both substituted and unsubstituted phenylene units must have some degree of partial double bond characters. This is as a result of the delocalized electrons of the phenylene rings which actually makes their C−C bond as one and a half bonds between the carbons, and it does make sense in reference to the experimentally reported bond length values. Contrastingly, the measured values for the interior (in the range of 114°) and the exterior (in the range of 123°) bond angles, and the concerned dihedral angles of the substituted and unsubstituted phenylene units in the X−ray, DFT, and SCC−DFTB derived structures of **1a**, **1b**, and **1c** are found to be deviated from the corresponding values of the original planar benzene molecule where each bond angle is fixed to 120° (all the interior and exterior bond angles are not mentioned in Table 1 because of their less significance).
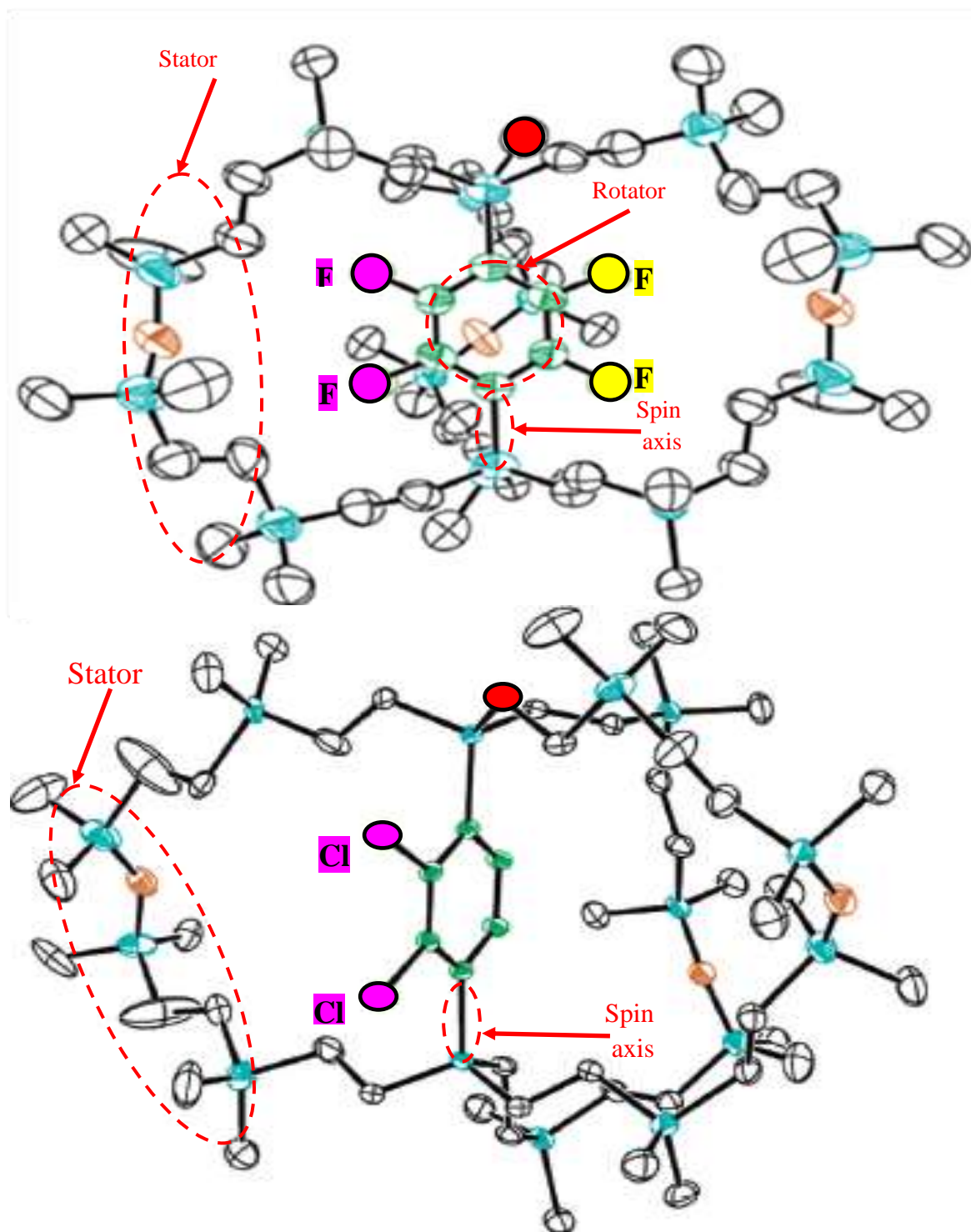
*Figure 2: X–ray crystallography of the crystalline siloxaalkane molecular gyroscopes (a) **1b** (ROT–2F) with two stable positions **A** and **B** of difluorophenylene rotator (indicated by yellow and pink spheroids), (b) **1c** (ROT–2Cl) with a single stable position of dichlorophenylene rotator (indicated by pink spheroids). Both of them are reproduced from the ref. 24. Hydrogen atoms and the structural disorder on the siloxaalkane chains are omitted for clarity. The phenylene dihedral angles in both of them are formed by the C atom of the arm (red spheroid), Si (blue)–C(green) of the spin axis, and the ortho C atom in phenylene.*

These notable angular distortions are as a result of the effect of vDW type intramolecular (interactions between the siloxaalkane arms and the central phenylene unit of each molecular gyroscope/compass) and intermolecular (interactions between the molecular gyroscopes/compasses present inside the unit cell) interactions. In the language of stereochemistry, the origination of these interactions are mostly due to the steric effects experienced by each molecular gyroscope/compass present in the respective unit cells of **1a**, **1b**, and **1c**: the repulsive forces between the overlapping electron clouds of the central phenylene unit and the surrounding siloxaalkane spokes, and the same type forces between the siloxaalkane arms of the same molecules and that of the nearby molecules arranged periodically to each other. In short, the steric type hindrance of each molecular gyroscope/compass **1a**, **1b**, and **1c** is mostly responsible to distort the internal shapes of their centrally located phenylene units as well as to impose them for occupying a particular site of the free space present inside the static siloxaalkane spokes. Similarly, if we closely observe their phenylene dihedral angles ϕ formed by the four specific atoms defined in Figure 1 and Figure 2, we can easily locate the exact position of the phenylene units inside the siloxaalkane spokes of **1a**, **1b**, and **1c**. As listed in Table 1, the phenylene dihedral angle for the X−ray produced most stable structure **B** of **1a** is 0.55π (modulo π), the difluorophenylene dihedral angle for the two degenerate X−ray derived equilibrium structures **A** and **B** of **1b** are 0.56π and 1.57π ($0.56\pi \leftrightarrow 1.57\pi$; 1π flip), and the dichlorophenylene dihedral angle for the one and only equilibrium structure of **1c** is 0.61π. By the SCC−DFTB method, these angles are converged to 0.35π, $0.60\pi \leftrightarrow 1.61\pi$ (1π flip), and 0.64π respectively under periodic boundary condition. These theoretically predicted data sets not only confirm the experimentally observed two degenerate positions of **1b** related to each other by 1π flipping (Figure 4 and Figure 5) but also declare the structural reproducibility of the X−ray derived unit cells of each molecular gyroscope/compass in the crystalline state (Figure 3 to Figure 6). Taking into account the precision of all the above mentioned theoretically produced structural data sets and the exact likeness of thus derived crystal structures with that of X−ray crystallography, the performance of the SCC−DFTB method is evaluated as extraordinary.

In their original research paper [24], Setaka *et al.* has reported a significant structural deformation more especially in the siloxaalkane arms of the molecular gyroscopes **1b** and **1c** in crystalline state where two hydrogen atoms of the central phenylene (as in **1a**) are substituted by two fluorine (as in **1b**) and two chlorine (as in **1c**) respectively. They emphasized that the deformed siloxaalkane spokes narrow down the free−volume units (the volume where the rotator is enclosed by the static framework inside which it moves more or less freely) available in **1b** and **1c** considerably than that exists in **1a** which results to show facile, restricted, and prevented type phenylene flipping as in **1a**, **1b**, and **1c** respectively. We have also confirmed these structural abnormalities theoretically in isolated molecular gyroscopes of **1b** & **1c**, and also interpreted them quantitatively through the series of DFT and DFTB based quantum mechanical methods [21], [30], [31]. Accordingly, we also applied these methods to **1a**, implemented them under periodic as well as non−periodic boundary conditions, and elucidated its experimentally observed structural and dynamical assets theoretically [20]. However, how actually (1) the structural variation in **1b** and **1c** takes place under PBC, and (2) the nature of phenylene flipping in **1b** and **1c** are made different; while inserting dipolar units such as 2F and 2Cl atoms in the central phenylene unit of **1a** are not revealed quantitatively. Beside this, the direct influence of the significantly deformed siloxaalkane spokes in localizing the central phenylene units of **1a**, **1b**, and **1c**, and their decisive role in demonstrating either smooth or restricted rotation as in **1a** and **1b** respectively or completely prevented rotation as in **1c** has not been depicted quantitatively through theoretical studies. Herein, we have clarified these issues in various ways.

It is quite obvious that the degree of intra−molecular interactions (interactions between the rotator and stator of each molecule present in each unit cell of each molecular gyroscope/compass) is relatively more whenever two bulkier halogen atoms are inserted into the central phenylene unit of **1a** as in **1b** and **1c**. This results to the increment in energy barrier experienced by both difluoro− and dichloro− substituted phenylene units of **1b** and **1c** while demonstrating internal rotary motion. Moreover, this interaction also subjects to widen the available space (free−volume) present around these units than that already present in molecular moiety **1a**. This side by side enlargement in the free−volume unit is also mostly favored by the flexible & bond stretching features of the Si−O

bonds plus the bending degrees of freedom of *Si−O−*Si *parts* of each siloxaalkane arm as verified experimentally through thermal induction method [24], [25]. As a whole, the free−volume units, rotational energy barriers, and the types of internal rotation (smooth, restricted, and prevented type as in **1a**, **1b**, and **1c** respectively) observed in all the three crystalline molecular gyroscopes/ compasses are correlated to each other significantly.
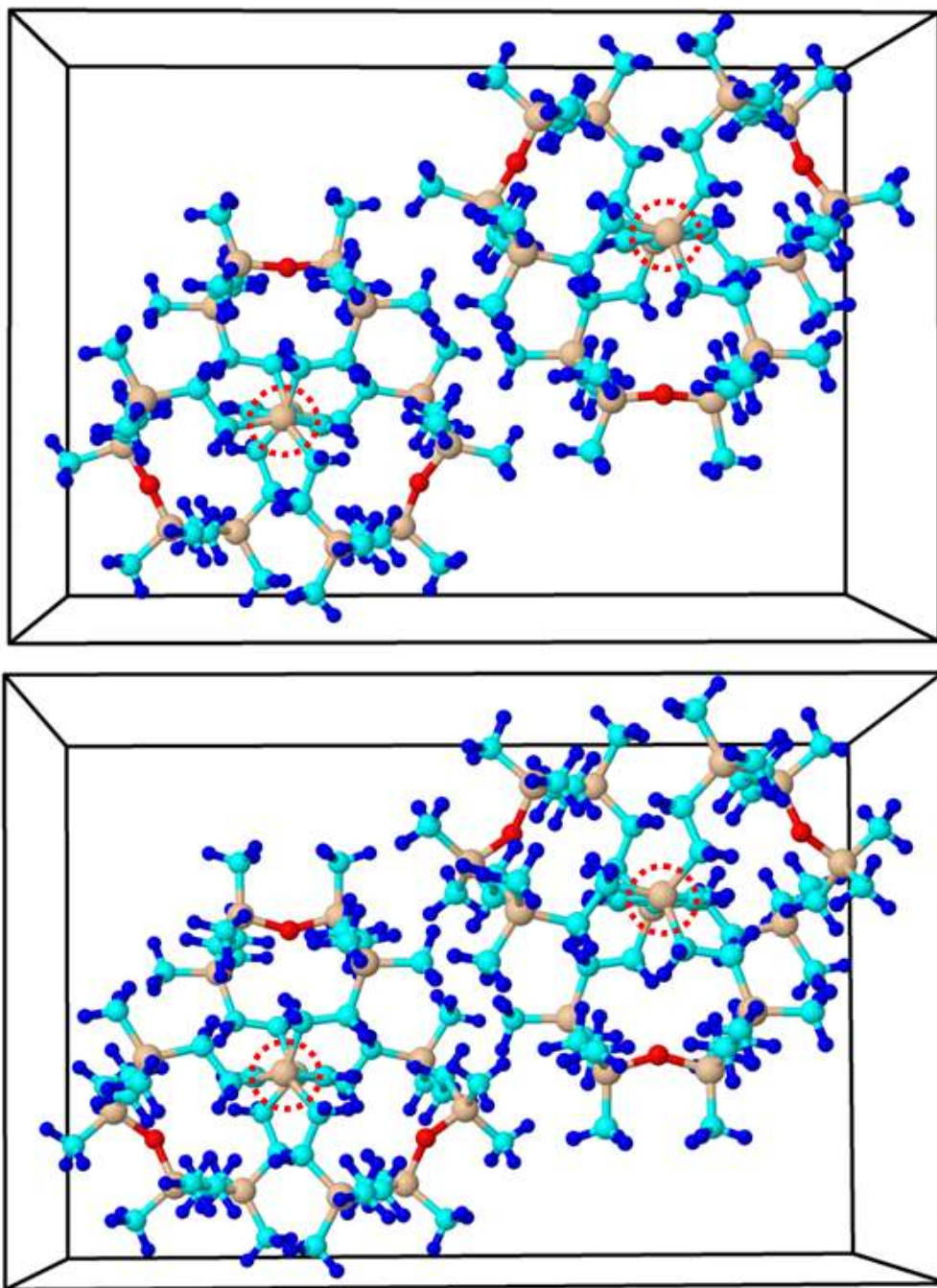

*Figure 3: (a) X−ray crystallography, (b) SCC−DFTB optimized unit−cell geometry of the most stable position (structure **B**) of the crystalline siloxaalkane molecular gyroscope **1a** (ROT− 2H). They are reproduced from the previous publication [ref. 20] of the same authors for structural comparison. The cyan, blue, dark gray, and red spheroids represent Carbon, Hydrogen, Silicon, and Oxygen atoms respectively. The two phenylene rotators of the unit−cells are enclosed in red circles.*
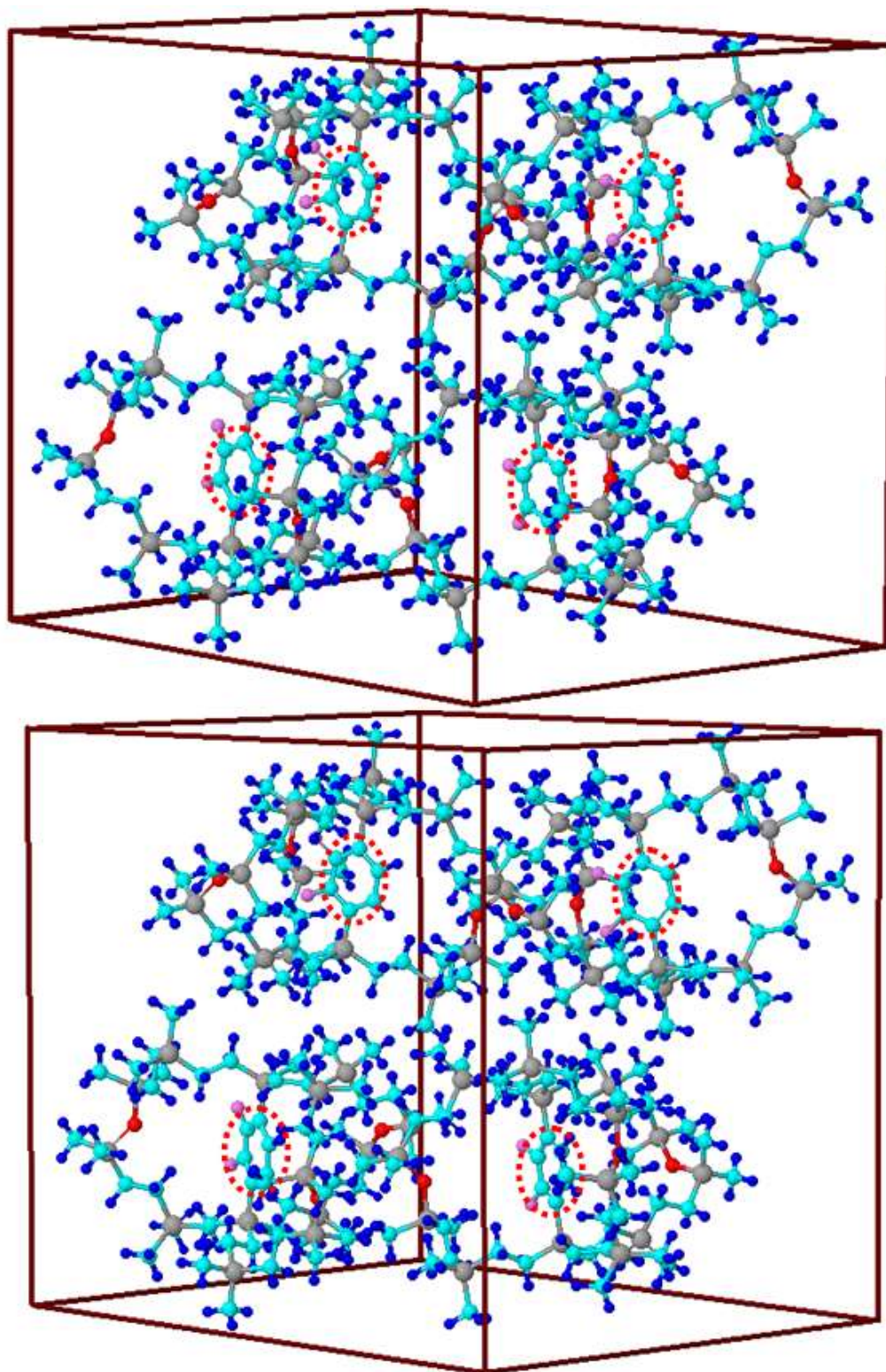
*Figure 4: (a) X−ray crystallography, (b) SCC−DFTB optimized unit−cell geometry (position **A**) of the crystalline siloxaalkane molecular gyroscope **1b** (ROT−2F). The cyan, blue, dark gray, red, and indigo spheroids represent Carbon, Hydrogen, Silicon, Oxygen, and Fluorine atoms respectively. The four phenylene rotators of the unit−cell are enclosed in red circles.*

In order to quantize this interdependence, we estimated the free−volume unit present around the rotating part of each molecular gyroscope/compass **1a**, **1b**, and **1c** by determining $[d_{CO}\{d_1, d_2, d_3\}]$ distance in their X−ray and DFTB derived ground state electronic structures. This measurable parameter $[d_{CO}\{d_1, d_2, d_3\}]$ actually approximates the intervening space exists in between O−atom of each siloxaalkane arm (there are in total three siloxaalkane arms) and the phenylene ortho carbon holding H−atom as in **1a**, F−atom as in **1b**, and Cl−atom as in **1c**. Each individual set of the $[d_{CO}\{d_1, d_2, d_3\}]$ values measured in the respective X−ray and SCC−DFTB derived equilibrium structures of all the three molecular gyroscopes/compasses are listed in the fourth column of Table 1. If we compare each of them with critical analysis, the concerned $[d_{CO}\{d_1, d_2, d_3\}]$ data set resembles quite well to each other except some minor irregularities. It makes us to claim that the SCC−DFTB derived ground state electronic structure of each unit cell of each molecular gyroscope/compass possesses as sufficient free−volume unit as in their respective X−ray crystallography. Meanwhile, the trend of each set of the $[d_{CO}\{d_1, d_2, d_3\}]$ values for three different molecular gyroscopes **1a**, **1b**, and **1c** are theoretically predicted in the order of: d_{CO} (**1a**) < d_{CO} (**1b**) < d_{CO} (**1c**). This increasing trend can be used to further quantify the experimentally observed structural deformation more especially in the siloxaalkane spokes of **1b** and **1c**. The most important conclusion we derived from here is: molecular gyroscope **1c** bears a large amount of free−volume unit followed by **1b**, and **1a** in their specific crystalline states. And, this dissimilar trend eventually reflects us that more bulky the rotating part is, more is the space (free volume) required to accommodate it inside the siloxaalkane spokes: the dichlorophenylene (atomic size of Cl: 0.99Å) in **1c** is the bulkiest unit, the difluorophenylene (atomic size of F: 0.64Å) in **1b** is the second most bulky unit, and the unsubstituted phenylene in **1a** is the smallest (atomic size of H: 0.37Å) unit. The more closely connected structural analogies with these bulkier rotating segments are their powerful strength in deforming peripheral siloxaalkane spokes: a dichlorophenylene in **1c** (the bulkiest unit) forces the siloxaalkane arms farther apart than that by difluorophenylene in **1b** (the second most bulky unit) and by phenylene in **1a**. This explanation leads to claim that **1c** feels more outward expansion (ballooning) of its spokes than that by **1b**, *i.e.* their gyroscopic siloxaalkane frameworks are subjected to distort more significantly from their original alignments present in the synthetic precursor module **1a**. Alternatively, the bulkier groups F & Cl attached to **1b** and **1c** respectively creates stronger steric effects to the surrounding siloxaalkane spokes than that endorsed by the phenylene−H atoms present in **1a**. This is actually a complementary electronic effect responsible to affix the definite shape of the entire molecular gyroscope/compass. It means the stronger steric repulsive forces between the dihalogen substituted bulky phenylene rotators and the surrounding siloxaalkane arms (as in **1b** and **1c**) make the spokes puffed out greatly. Thus, the steric hindrance is also one of the most important considerable factors in designing gyroscopic molecular structures as it can create repulsive type forces which induce the internal structure to attain sufficient free−volume unit centrally. This is of course a very essential strategic part while designing and synthesizing gyroscopic structures having completely closed topology.

Again, the steric interactions between the central rotating unit and the surrounding siloxaalkane arms, interactions between the arms themselves, and the interactions between the molecules present in each unit cell also influences the rotational energy barrier; a decisive parameter in predicting how smoothly **1a**, **1b**, and **1c** demonstrate rotary motions. Actually, they are correlated to each other: stronger interactive forces always result to higher energy barrier Ea faced by the rotating unit, and this Ea in principle determines whether the rotating segment shows smooth, and hindered rotations or not (prevented rotations) at ordinary temperatures as observed experimentally in **1a**, **1b** and **1c** respectively. As a rule, the weaker intra− and inter− molecular interactions always result to significantly low Ea implying that the rotating unit demonstrates smooth type rotation even at room temperature (T = 300 K) as observed in **1a** experimentally [23] and theoretically (DFTB−MD simulation) [20]. From this logical interpretations, we can predict **1a < 1b < 1c** trend of the energy barriers experienced by their rotating units, which in turn describes why their respective rotating segments phenylene, difluorophenylene, and dichlorophenylene exhibit facile (low rotational barrier), restricted (comparatively high rotational barrier), and prevented (comparatively higher rotational barrier) type flipping motions at ordinary temperatures. Accordingly, based on the SCC−DFTB predicted crystal

structures and the unit cell closed− packings of the molecules (Figure 3 to Figure 5), the appropriateness and the favorability of the crystalline molecular gyroscopes/compasses **1a**, **1b**, and **1c** for exhibiting rotary motion are also elucidated here.
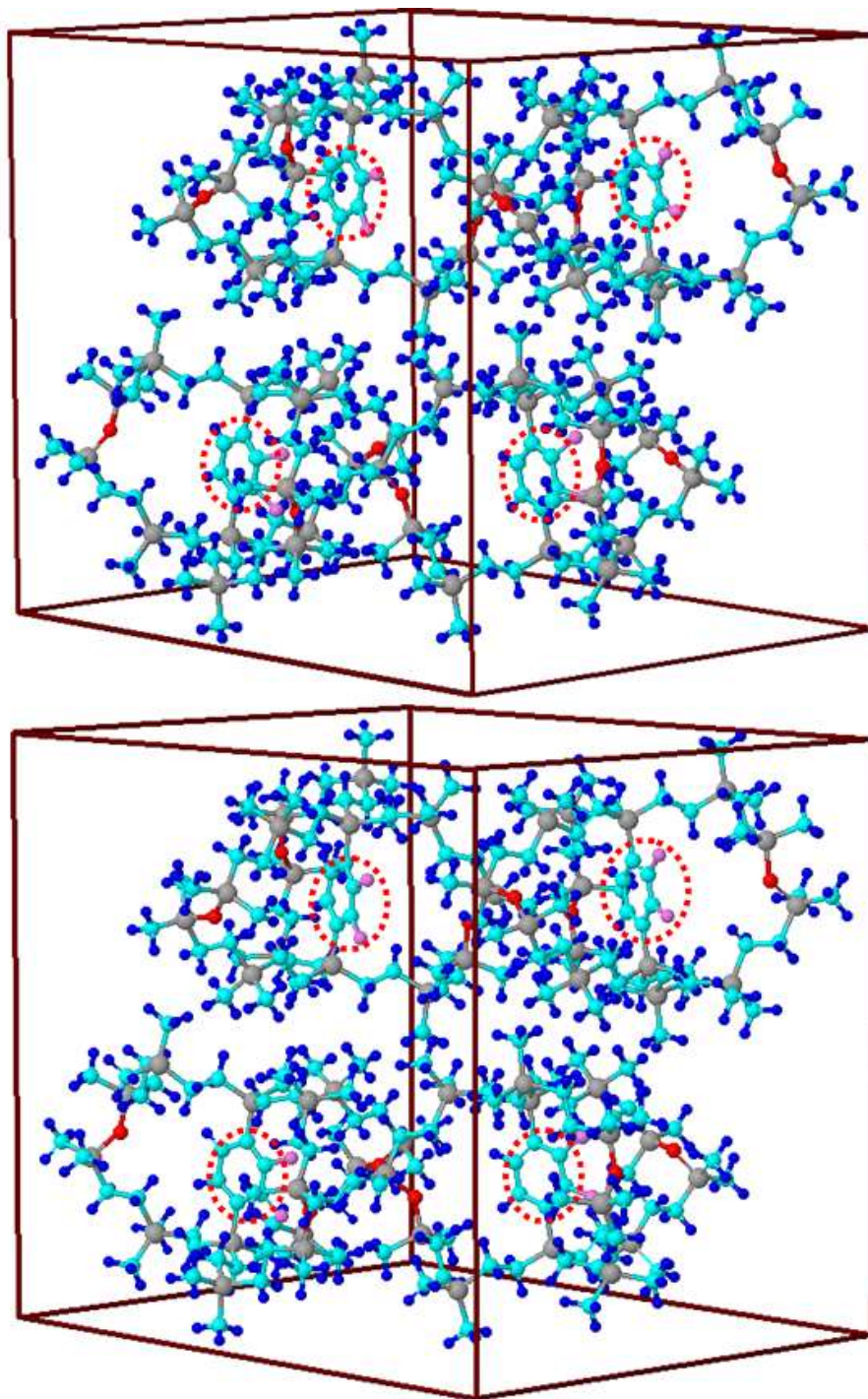

*Figure 5: (a) X−ray crystallography, (b) SCC−DFTB optimized unit cell geometry (position **B**) of the crystalline siloxaalkane molecular gyroscope **1b** (ROT−2F). The cyan, blue, dark gray, red, and indigo spheroids represent Carbon, Hydrogen, Silicon, Oxygen, and Fluorine atoms respectively. The four difluorophenylene rotators of the unit−cell are enclosed in red circles*
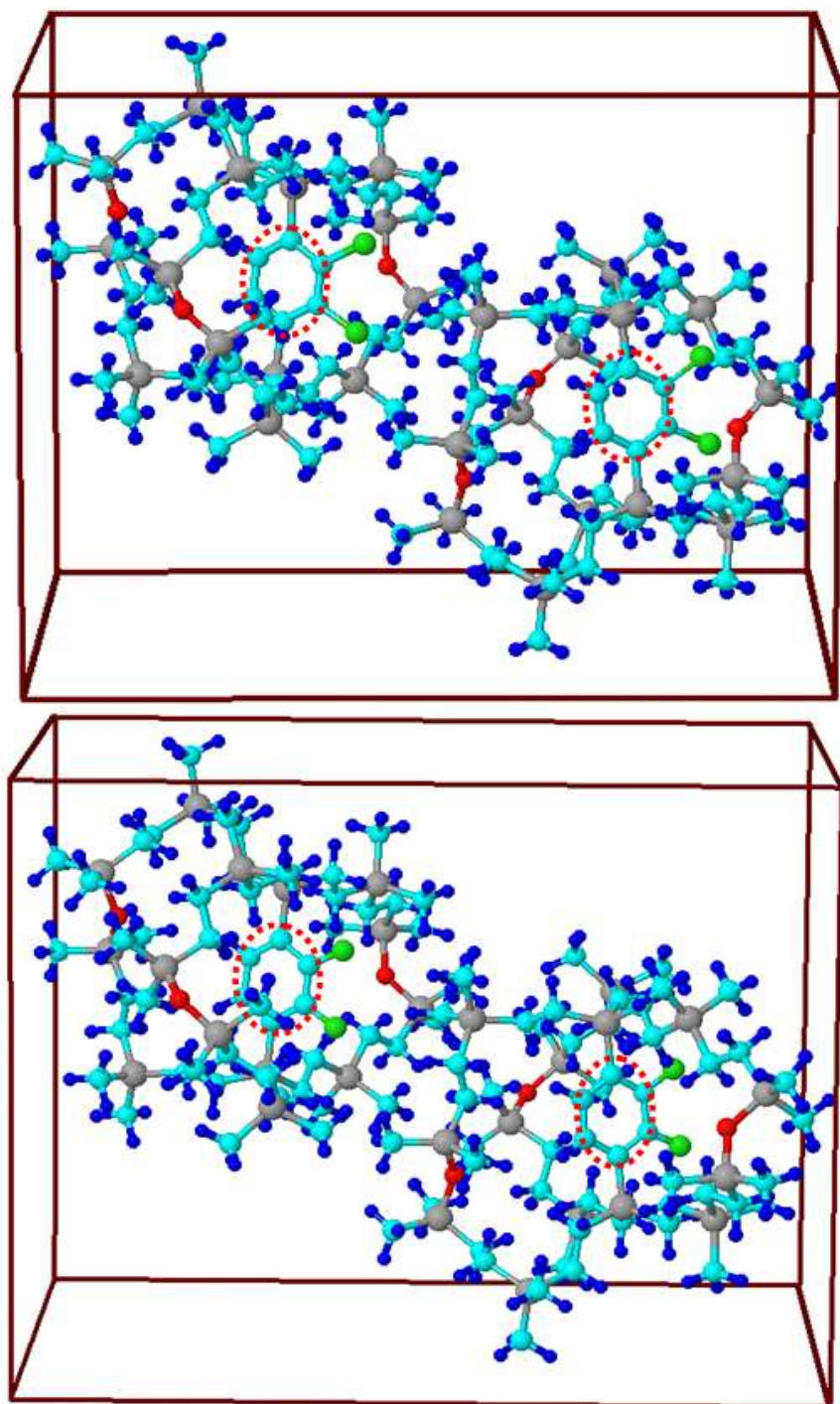
*Figure 6: (a) X–ray crystallography, (b) SCC–DFTB optimized unit cell geometry of the crystalline siloxaalkane molecular gyroscope **1c** (ROT–2Cl). The cyan, blue, dark gray, red, and green spheroids represent Carbon, Hydrogen, Silicon, Oxygen, and Chlorine atoms respectively. The two dichlorophenylene units of the unit–cell are enclosed in red circles.*

As can be seen in SCC−DFTB derived crystal structure of **1c** in Figure 5, it looks inappropriate to behave as amphidynamic crystal due to the obstruction of its dichlorophenylene segment for showing 1,4−axial rotation caused by the unfriendly orientations of the peripheral siloxaalkane arms. In the support of this non−amphidynamic feature, the restricted position of the central non planar dichlorophenylene unit and the inappropriate orientation of its two Cl atoms towards each siloxaalkane arm remains as good evidences. In contrast to this, the SCC−DFTB produced unit cell structures of **1a** (Figure 3), and **1b** (Figure 4) clearly display very friendly orientations of the central rotating units and their surrounding siloxaalkane arms in the three dimensional space. Exactly same structural differences especially in the positions of the peripheral siloxaalkane arms are reported by Setaka *et al.* as well. All these semiquantitatively reproduced theoretical justifications have illuminated the exceptional potentialities of the SCC−DFTB method in featuring rotary dynamics including rotational energy barriers of **1b** and **1c** type crystalline gyroscopic molecular assemblies under PBC. Present authors are currently proceeding this research project.

Table 2. Experimental vs. Theoretical structural parameters for each siloxaalkane arm of the molecular gyroscopes **1a**, **1b**, and **1c** in their unit cell structures

Molecular gyroscopes	Si−O−Si angle (θ) (π)		Bonds	Bond lengths (Å)	
	X−ray	**SCC-DFTB**		**X−ray**	**SCC-DFTB**
1a			C−C	1.6	1.5
(ROT−2H)	0.90	0.80	C−H	1.0	1.1
	0.96	0.79	C−Si	1.9	1.9
	0.94	0.83	Si−O	1.6	1.7
1b			C−C	1.5	1.5
(ROT−2F)	0.96	0.79	C−H	0.9	1.1
Structure **A**	0.84	0.75	C−Si	1.9	1.9
	0.84	0.75	Si−O	1.6	1.7
Structure B			C−C	1.4	1.5
	0.97	0.79	C−H	0.9	1.1
	0.84	0.75	C−Si	1.9	1.8
	0.84	0.74	Si−O	1.6	1.7
1c			C−C	1.5	1.5
(ROT−2Cl)	0.79	0.74	C−H	1.1	1.1
	0.80	0.76	C−Si	1.8	1.9
	0.83	0.79	Si−O	1.7	1.7

According to the report published by Setaka *et al.* elsewhere [23, 24], three chemically identical siloxaalkane arms of each molecular gyroscope/compass **1a**, **1b**, and **1c** are highly flexible and stretching type due to −(Si−O)$_x$− bonds and their chains & segments. The most notable advantage of these features is to ease the arms in encapsulating differently sized rotating units such as phenylene as in **1a**, difluorophenylene as in **1b**, and dichlorophenylene as in **1c** through quick structural adjustment. Such type features are in fact quite essential in strategic synthetic process of completely closed−topological crystalline macrocages while making their arms dilating inward and outward whenever required. Setaka *et al.* have claimed these unique features of silicone based molecular gyroscopes/compasses as quite indispensable part more especially for enhancing the inherent strength & conformational flexibility of the peripheral spokes and the pronounced pliability of the whole gyroscopic molecules and also for functionalizing them through the externally controlled electrical, thermal and optical responses. The feasibility of such type induction mechanisms is actually made more practicable due to the extra thermal stabilities, higher temperature resistivities, and the notable bond dissociation energy E_B of −(Si−O)$_x$− segments (E_B for Si−O bonds, C−C bonds, C−O bonds are 108 kcal mol^{-1}, 82.6 kcal mol^{-1}, 85.2 kcal mol^{-1} respectively) [36]. More specifically, the most closely associated consequence of such extraordinary features is to maintain widely varied free−volume units around the differently sized rotating units as approximated earlier by the DFTB computed

$[d_{CO}\{d_1, d_2, d_3\}]$ sets for **1a**, **1b**, and **1c** as well. Therefore, one more indirect way to quantify the free−volume unit of each molecular gyroscope/compass is by determining all the concerned bond angles and bond lengths associated to the $-(\text{Si}-\text{O})_x-$ segments such as C−C, C−Si, C−H, Si−O bond lengths and Si−O−Si bond angles of each arm. Side by side, these structural data sets elucidate how closely the computationally produced electronic structures resembled with their X−ray produced counterparts. These structural parameters for both X−ray and SCC−DFTB derived unit cell structures of **1a**, **1b**, and **1c** are summarized in Table 2. Interestingly, no remarkable changes in the bond lengths associated with the C atoms of each arm are observed. Moreover, there are no big variations in the bond lengths listed in Table 2 while accommodating bulkier rotating segments such as difluorophenylene (as in **1b**) and dichlorophenylene (as in **1c**). In difference to this, all the Si−linked bond lengths and bond angles such as $-(\text{Si}-\text{O})_x-$ chains and Si−O−Si linkages of each siloxaalkane arm are, however, found to vary significantly. This variation is more intense in the Si−O−Si bond angles; even relatively more acute in the SCC−DFTB converged structures in comparison to the X−ray crystallography. However, this diverseness in Si−O−Si bond angles and $-(\text{Si}-\text{O})_x-$ bond lengths are theoretically acceptable if the partial ionic and double bond characters of them are recognized in terms of their quantum mechanical treatments [37]. Similarly, if we compare the Si−O−Si bond angles among the molecular gyroscopes/compasses, the **1b** and **1c** have more acute angles than those in **1a**. This further ascertains that bulkier difluorophenylene and dichlorophenylene units of **1b** and **1c** respectively repel their surrounding arms more strongly (steric hindrance) than that does by the phenylene unit of **1a**. In other words, the intense steric hindrance created by the two F and two Cl atoms attached to the central phenylene unit force the surrounding siloxaalkane arms outward resulting a significant reduction in the Si−O−Si bond angles but considerable increments in the free−volume units. In terms of all other perspectives except to these abnormalities caused by the $-(\text{Si}-\text{O})_x-$ segments of each siloxaalkane arm, the SCC−DFTB optimized and the X−ray produced unit cells of all the three molecular gyroscopes are in good agreement structurally. As shown in Figure 3 to Figure 6, the structural orientations and the spatial distribution of the siloxaalkane arms and their substituent groups such as Si−CH₃, Si−O etc. of each molecule present in the unit cell of each crystalline molecular gyroscope/compass are also quite unanimous. All the notable results and discussions presented above triggered the DFTB+ computational scheme in advancing and promoting SCC−DFTB method towards the structural and dynamical characterizations of the giant crystalline molecular assemblies.

As a whole, all the aforementioned exceptional performance of the SCC−DFTB method while applying to the experimentally synthesized amphidynamic type crystalline molecular gyroscopes/compasses eventually boosts up this mathematical scheme to the level of computationally cheap yet most efficient and decent quantum mechanical method. We are expecting same level precisions while computing experimentally unpredicted parameters such as rotational energy barriers, temporal behavior of the phenylene rotational angles and the phenylene flipping motions, time dependent flipping rates, and the detailed consequences of the rotary dynamics of each molecular gyroscope/compass under crystalline molecular condition. In the same context, we are currently proceeding SCC−DFTB investigations of the crystalline molecular compass **1b** with the theme of computing: (1) rotational potential energy surfaces with activation energies Ea, 1π−flipping positions of the two degenerate equilibrium structures, and their concerned ground state electronic geometries, and (2) flipping barrier experienced by the central rotating unit through the Gaussian−external methodology, and (3) temporal behavior of the flipping motions and the flipping rates of the rotator at wide ranged kinetic temperatures (T = 300K to 1200K) through DFTB−MD simulations. To those research scholars who are interested to know in−depth about these issues for the crystalline molecular gyroscope **1a**, the prospective research papers published by the same authors elsewhere [20], [21], [22], [30], [31] are recommended.

4. Conclusion

This theoretical research work was mainly aimed at characterizing the ground state electronic structures of the experimentally synthesized crystalline siloxaalkane molecular compasses (gyroscopes) encapsulating dihalogen substituted polar (nonpolar) phenylene units. The molecular compasses of our subject of major interest were named

as ROT−2F and ROT−2Cl due to having difluorophenylene and dichlorophenylene segments as polar rotators (compass needles) respectively at the central position and three chemically identical siloxaalkane arms in each as static spokes at the peripheral positions. And, the molecular gyroscope we referred here is none other than their own molecular analogue and synthetic precursor module ROT−2H with a central nonsubstituted phenylene as a rotating unit surrounded peripherally by the exactly same type spokes. The potential theoretical method of our choice was SCC−DFTB scheme implemented *in* the *DFTB+* code due to its tremendous abilities in computing electronic properties of the crystalline molecular systems under periodic boundary condition. In this theoretical insight, the relatively better approaches of the SCC−DFTB method for characterizing the X−ray crystallography of ROT−2H, ROT−2F, & ROT−2Cl as well as for elucidating the significant roles of their three dimensional crystal structures in showing amphidynamic behavior (smooth, restricted, and prevented type phenylene rotation respectively) in the crystalline state were presented.

Herein, we basically examined all the X−ray produced stable structures of the three different crystalline molecular compasses/gyroscopes quantum mechanically: for ROT−2H, the most stable X−ray observed unit cell structure (out of its three stable forms); for ROT−2F, both of the degenerate unit cell structures (structure **A** and **B**); and for ROT−2Cl, a single stable unit cell structure were optimized individually under SCC−DFTB periodic boundary condition (PBC). The computationally converged unit−cell structures of each of them were fully characterized on the basis of explicitly measured structural data sets: bond lengths, bond angles and dihedral angles associated with both central rotating segments as well peripheral siloxaalkane arms of each experimentally and theoretically derived ground state electronic structures. Interestingly, no prominent structural abnormalities in their SCC−DFTB derived unit−cells were observed while referring to the same data sets for their own X−ray crystallography. However, in each of them, the Si−O bond lengths and the concerned bond angles linked to $-(Si-O)_x-$ segments and Si−O−Si linkages of all the three siloxaalkane arms were found to vary significantly, which in fact lies in the agreeable range if the recognition of double bond and partial ionic characters in them are considered on the basis of the mathematical approximations made during the development of quantum mechanical algorithms of the DFTB. Accordingly, the available "free−volume" unit present around the central rotating segment of each molecule present in the unit−cell of each molecular gyroscope/compass was confirmed by measuring theoretically predicted $d_{CO}\{d_1, d_2, d_3\}$ datasets (they actually measure an intervening space exists in between O−atom of each siloxaalkane arm and the phenylene ortho carbon holding halogen atoms). We also used each set of these $d_{CO}\{d_1, d_2, d_3\}$ values for the quantitative interpretation of experimentally observed structural deformation more especially in the structures of the siloxaalkane spokes of ROT−2F and ROT−2Cl, and found as reasonable agreement as experimental observation. While analyzing theoretically derived unit−cell structures and the overall molecular geometries critically, we concluded that the steric hindrance and intra−molecular type Van der waals force of interactions between the centrally located phenylene segments and their respective peripheral arms are among the few major descriptors responsible to justify experimentally reported notable structural deformation and centrally exists free−volume units in each molecular gyroscope/compass semiquantitatively. Beside this, the extent of change in free−volume units of ROT−2H while inserting bulkier dipolar difluoropheylene and dichlorophenylene segments centrally (as in ROT−2F and ROT−2Cl) is mainly recognized as a fundamental basis for interpreting experimentally reported smooth, restricted, or prevented type phenylene rotation in crystalline state.

Acknowledgement

Notes

The authors declare no competing financial interest.

References

[1]. W. Kohn, L. J. Sham, "Self-consistent equations including exchange and correlation effects", *Physical Review*, Vol. 140, No. 4A, pp. A1133–A1138, 1965.

[2]. A. B. Marahatta, "A DFT Analysis for the Electronic Structure, Mulliken Charges Distribution and Frontier Molecular Orbitals of Monolayer Graphene Sheet", *International Journal of Progressive Sciences and Technologies*, Vol. 16, No. 1, pp. 51–65, 2019.

[3]. P. Hohenberg, W. Kohn, "Inhomogeneous Electron Gas", *Physical Review B*, Vol. 136, No. 3B, pp. 864–871, 1964.

[4]. A. B. Marahatta, "DFT Study on Ground State Electronic Structures of Simple to Complex Molecular Specimens", *International Journal of Progressive Sciences and Technologies*, Vol. 19, No. 1, pp. 100–112, 2020.

[5]. A. J. Cohen, P. M. Sánchez, W. Yang, "Insights into current limitations of density functional theory" *Science*, Vol. 321, Issue 5890, pp. 792–794, 2008.

[6]. D. Buckingham, P. W. Fowler, J. M. Hudson, "Theoretical studies of van der Waals molecules and intermolecular forces", *Chemical Reviews*, Vol. 88, No. 6, pp. 963–988, 1988.

[7]. J. Tao, J. P. Perdew, A. Ruzsinszky, "Accurate van der Waals coefficients from density functional theory", *Proceedings of the National Academy of Sciences of the U. S. A.*, Vol 109, Issue 1, pp. 18–21, 2012.

[8]. A. D. Becke, "Density-functional thermochemistry. III. The role of exact exchange", *Journal of Chemical Physics*, Vol. 98, Issue 7, pp. 5648–5652, 1993.

[9]. J. P. Perdew, K. Burke, M. Ernzerhof, "Generalized Gradient Approximation Made Simple", *Physical Review Letter*, Vol. 77, pp. 3865–3868, 1996.

[10]. J. Tao, J. P. Perdew, V. N. Staroverov, G. E. Scuseria, " Climbing the density functional ladder: nonempirical meta-generalized gradient approximation designed for molecules and solids", *Physical Review Letter*, Vol. 91, Issue 14, *146401-1*–146401-4, 2003.

[11]. G. Seifert, "Tight-Binding Density Functional Theory: An Approximate Kohn−Sham DFT Scheme", *Journal of Physical Chemistry A*, Vol. 111, Issue 26, pp. 5609–5613, 2007.

[12]. G. Zheng, S. Irle, K. Morokuma, "Performance of the DFTB method in comparison to DFT and semiempirical methods for geometries and energies of C_{20}–C_{86} fullerene isomers", *Chemical Physics Letter*, Vol. 412, Issue 1–3, pp. 210–216, 2005.

[13]. B. Aradi, B. Hourahine, Th. Frauenheim, "DFTB+, a Sparse Matrix-Based Implementation of the DFTB Method", *Journal of Physical Chemistry A*, Vol. 111, Issue 26, pp. 5678–5684, 2007.

[14]. M. Elstner, D. Porezag, G. Jungnickel, J. Elsner, M. Haugk, Th. Frauenheim, S. Suhai, G. Seifert, " Self-consistent-charge density-functional tight-binding method for simulations of complex materials properties", *Physical Review B*, Vol. 58, pp. 7260–7268, 1998.

[15]. T. Frauenheim, G. Seifert, M. Elstner, T. Niehaus, C. Köhler, M. Amkreutz, M. Sternberg, Z. Hajnal, A. D.Carlo, S. Suhai, " Atomistic simulations of complex materials: ground-state and excited-state properties", *Journal of Physics: Condensed Matter*, Vol. 14, pp. 3015–3047, 2002.

[16]. Koehler, Z. Hajnal, P. Deak, Th. Frauenheim, S. Suhai, "Theoretical investigation of carbon defects and diffusion in α-quartz", *Physical Review B*, Vol. 64, pp. 085333, 2001.

[17]. M. Elstner, Th. Frauenheim, E. Kaxiras, G. Seifert, S. Suhai, "A Self-Consistent Charge Density-Functional Based Tight-Binding Scheme for Large Biomolecules", *Physical Status Solidi B,* Vol. 217, Issue 1, pp. 357–376, 2000.

[18]. M. Elstner, P. Hobza, Th. Frauenheim, S. Suhai, E. Kaxiras, "Hydrogen bonding and stacking interactions of nucleic acid base pairs: A density-functional-theory based treatment", *Journal of Chemical Physics*, Vol. 114, Issue 12, pp. 5149–5155, 2001.

[19]. E. Rauls, R. Gutierrez, J. Elsner, Th. Frauenheim, "Stoichiometric and non-stoichiometric (1010) and (1120) surfaces in 2H–SiC: a theoretical study", *Solid State Communications*, Vol. 111, Issue 8, pp. 459–464, 1999.

[20]. A. B. Marahatta, M. Kanno, K. Hoki, W. Setaka, S. Irle, H. Kono, "Theoretical Investigation of the Structures and Dynamics of Crystalline Molecular Gyroscopes", Journal *of Physical Chemistry C*, Vol. 116, pp. 24845–24854, 2012.

[21]. A. B. Marahatta, H. Kono, "Performance of NCC- and SCC-DFTB Methods for Geometries and Energies of Crystalline Molecular Gyroscope", *International Journal of Innovative Research and Advanced Studies*, Vol. 6, Issue 5, pp. 180–185, 2019.

[22]. A. B. Marahatta, "Geometry Optimization Skills of DFTB: Simple to Complex Molecular Systems", *International Journal of Progressive Sciences and Technologies*, Vol. 15, No. 2, pp. 263–277, 2019.

[23]. W. Setaka, S. Ohmizu, C. Kabuto, M. Kira, "A Molecular Gyroscope Having Phenylene Rotator Encased in Three-Spoke Silicon-Based Stator", *Chemistry Letter*, Vol. 36, pp. 1076–1077, 2007.

[24]. W. Setaka, S. Ohmizu, M. Kira, "Molecular gyroscope having a halogen-substituted *p*-phenylene rotator and silaalkane chain stators", *Chemistry Letter*, Vol. 39, pp. 468–469, 2010.

[25]. W. Setaka, K. Yamaguchi, "Thermal modulation of birefringence observed in a crystalline molecular gyrotop", *Proceedings of the National Academy of Sciences of the U. S. A.*, Vol. 109, pp. 9271–9275, 2012.

[26]. V. Balzani, M. Venturi, A. Credi, "*Molecular Devices and machines: A Journey into the Nano World*", Wiley-VCH: Weinheim, 2003.

[27]. A. Ehnbom, J. A. Gladysz, "Gyroscopes and the Chemical Literature, 2002−2020: Approaches to a Nascent Family of Molecular Devices", *Chemical Reviews*, Vol. 121, pp. 3701−3750, 2021.

[28]. Z. Dominguez, H. Dang, M. J. Strouse, M. A. Garcia-Garibay, "Molecular compasses and gyroscopes. III. Dynamics of a phenylene rotor and clathrated benzene in a slipping-gear crystal lattice", *Journal of American Chemical Society*, Vol. 124, Issue 26, pp. 7719–7727, 2002.

[29]. R. D. Horansky, L. I. Clarke, J. C. Price, T. V. Khuong, P. D. Jarowski, M. A. Garcia-Garibay, "Dielectric response of a dipolar molecular rotor crystal", *Physical Review B*, Vol. 72, pp. 014302-1–014302-5, 2005.

[30]. A. B. Marahatta, H. Kono, "Comparative Theoretical Study on the Electronic Structures of the Isolated Molecular Gyroscopes with Polar and Nonpolar Phenylene Rotator", *International Journal of Progressive Sciences and Technologies*, Vol. 20, No. 1, pp. 109–122, 2020.

[31]. A. B. Marahatta, H. Kono, "Structural Characterization of Isolated Siloxaalkane Molecular Gyroscopes via DFTB-based Quantum Mechanical Model", *International Journal of Progressive Sciences and Technologies*, Vol. 26, No. 1, pp. 526–541, 2021.

[32]. Jmol: an open-source Java viewer for chemical structures in 3D. *http://www.jmol.org/*

[33]. DFTB+ manual. *https://dftbplus.org/fileadmin/DFTBPLUS/public/dftbplus/latest/manual. pdf*

[34]. Y. K. Kang and M. S. Jhon, "Additivity of atomic static polarizabilities and dispersion coefficients", *Theoretica Chimica Acta*, Vol. 61, pp. 41–48, 1982.

[35]. K. J. Miller, "Additivity methods in molecular polarizability", *Journal of American Chemical Society*, Vol. 112, pp. 8533–8542, 1990.

[36]. R. G. Jones, W. Ando, J. Chojnowski, "Silicon-Containing Polymers: The Science and Technology of Their Synthesis and Applications", Springer publication, 2001.

[37]. M. Fujiki, J. R. Koe, K. Terao, T. Sato, A. Teramoto, J. Watanabe, "Optically Active Polysilanes. Ten Years of Progress and New Polymer Twist for Nanoscience and Nanotechnology", *Polymer Journal*, Vol. 35, pp. 297–344, 2003.